

Stochastic Engrams for Efficient Continual Learning with Binarized Neural Networks

Isabelle Aguilar^{a,*}, Luis Fernando Herbozo Contreras^a, Omid Kavehei^a

^a*School of Biomedical Engineering, The University of Sydney, NSW, 2006, Australia*

Abstract

The ability to learn continuously in artificial neural networks (ANNs) is often limited by catastrophic forgetting, a phenomenon in which new knowledge becomes dominant. By taking mechanisms of memory encoding in neuroscience (aka. engrams) as inspiration, we propose a novel approach that integrates stochastically-activated engrams as a gating mechanism for meta-plastic binarized neural networks (*mBNNs*). This method leverages the *computational efficiency of mBNNs* combined with *the robustness of probabilistic memory traces* to mitigate forgetting and maintain the model's reliability. Previously validated metaplastic optimization techniques have been incorporated to enhance synaptic stability further. Compared to baseline binarized models and benchmark fully connected continual learning approaches, our method is the only strategy capable of reaching average accuracies over 20% in class-incremental scenarios and achieving comparable domain-incremental results to full precision state-of-the-art methods. Furthermore, we achieve a significant reduction in peak GPU and RAM usage, under 5% and 20%, respectively. Our findings demonstrate **(A)** an improved stability *vs.* plasticity trade-off, **(B)** a reduced memory intensiveness, and **(C)** an enhanced performance in binarized architectures. By uniting principles of neuroscience and efficient computing, we offer new insights into the design of scalable and robust deep learning systems.

Keywords: Continual Learning, Engrams, Binarized Neural Networks, Metaplasticity

*Corresponding author: iagu0459@uni.sydney.edu.au

1. Introduction

Machine learning (ML) has made remarkable advances in solving complex problems across various domains, from natural language processing to autonomous systems. These successes have been primarily driven by the training and fine-tuning neural networks on large, static and retrospective datasets. However, in dynamic and prospective environments where data arrives sequentially - often in time-sensitive and real-time applications - these networks commonly face a fundamental limitation called catastrophic forgetting. Artificial neural networks (ANNs) usually lose previously acquired knowledge when training on new tasks. They often cannot adapt to incoming data, making them unsuitable for applications necessitating continual learning, such as implantable medical devices with closed-loop feedback, where strong energy constraints, wireless data telemetry bandwidth, and onboard memory capacity are crucial. These applications also exist in other domains where local data processing is optional, for example, on edge devices with adaptive response needs or closed-loop feedback, or necessary, for instance, on autonomous unmanned underwater vehicles for civil and defense purposes where any signal emission or communication is either undesired or impossible. In most cases, these operations also have long-term durations in which the device experiences new and unseen environments, furthering the importance of continual learning.

In contrast, neural systems possess an extraordinary ability to learn continuously, retaining memories while integrating new information. To address this discrepancy between artificial and biological networks, many brain-inspired approaches have been investigated [1, 2, 3]. Continual learning methods typically fall under five categories below [4], which can all potentially overlap with each others: (1) regularization-based approaches [5, 6, 7], (2) rehearsal or replay-based approaches [8, 9, 10], (3) architectural-based approaches [11, 12], (4) optimization-based approaches [13, 14], and (5) representation-based approaches [14, 15].

Metaplasticity, or the plasticity of synaptic plasticity, is a neuro-biological plasticity modulator, also shortly described as the "plasticity of synaptic plasticity" [16]. This biological mechanism regulates plasticity by influencing synaptic states and how adaptive the brain may be to incoming information. This ability is essential to balance varying strengths of synapses to stabilize incoming knowledge to the brain while allowing and adapting to new memories. This process is an attractive application as a regularization or

optimization approach to ANNs and has been proven successful as a method for continual learning compared to baseline feedforward networks [3, 17].

Another key mechanism in the brain is the formation and recall of engrams, sparse memory traces that encode, consolidate, and retrieve specific memories [18]. These neural ensembles are sparsely distributed across the brain and play a crucial role in recalling past information; in rodent-based experiments, activating the engram has been found to cue memory retrieval [19, 20]. Engrams are also closely related to associative learning, a fundamental study in neuroscience and psychology that has been investigated for years, including the notable classical conditioning of Pavlov’s dog [21]. In neuroscience, associative learning interprets how stimulus representations in the brain (formed by cues, environmental contexts, temporal information, etc.) inform behavioral outcomes [22]. As memories and information continue to stream into the brain, associated contexts assist in forming engrams, updating our biological neural networks, and adapting to incoming representations [23]. Furthermore, the brain has long been viewed as a stochastic system, and more recent studies have even proposed this stochasticity enhances associative memories and retention [24, 25].

These biological processes have parallels and inspired methods of deep learning. For example, the individual networks within an ensemble network approach could be considered separate engrams [26]. Engrams may be an emergent behavior in sparse neural networks, as we may observe the groups of neurons that remain active during learning as a memory trace for that task [27, 28]. Transfer learning and recurrent neural networks (RNNs) have associative memory mechanisms that improve storage and performance to traditional multilayer perceptions (MLPs) [29, 30]. Stochastic neural networks also exist, in which activations are no longer deterministic but follow a probabilistic distribution [31]. The most direct application of engrams and associative learning to continual learning methods may be using context-dependent gating to allocate neuronal ensembles [32, 33]. As it manipulates the neurons within a network, the application of engrams to neural networks most aligns with an architectural based approach. However, none of these methods have focused on implementing a model in resource-constrained environments.

In the ML field, binarized neural networks (BNNs) have emerged as a competitive alternative to their full-precision counterparts [34, 35, 36]. These one-bit networks show promise in producing a low-power solution to the catastrophic forgetting problem. We have developed a continual learning

approach that unifies the computationally efficient BNN with neuroscience-inspired learning mechanisms. Fig. 1 illustrates the biological mechanisms that motivated the engramBNN model. We demonstrate lifelong learning capability and model stability with multi-task domain-incremental and class incremental experiments using benchmark datasets such as Split-MNIST and CORe50 [37].

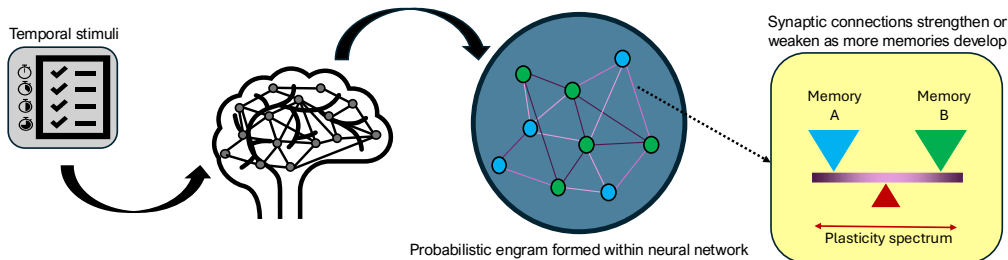


Figure 1: Continual learning mechanisms in biological and artificial networks. In the brain, experiences and stimuli are inputted into the system, forming engrams that encode and consolidate this information. As incoming memories flood the network, metaplasticity and synaptic plasticity allow the brain to adapt to additional knowledge and form corresponding engrams (green and blue) that interact or activate during memory recall. This process repeats throughout life, allowing continual learning capability in our brains.

2. Methods

2.1. Binarized Neural Network

Binarized neural networks (BNNs) are bit-wise versions of the standard MLPs that have dramatically reduced memory and energy usage, although these networks can produce similar and even improved performance compared to full-precision models [38, 39]. Unlike typical feedforward networks, the activations and weights of a BNN are bounded to $\{-1, +1\}$. Backpropagation occurs on a real-valued weight that influences gradient updates. However, the evaluation stage uses the binary weight, which is equal to the sign of the real-valued weight (aka. the "hidden weight").

Our model utilizes a network with two hidden layers, with 2048 neurons on each layer. For more stable training, batch-normalization is added after each layer [34]. The real-valued hidden weights are initialized over a uniform distribution between the values $[-0.5, 0.5]$.

2.2. Engram Gating Block

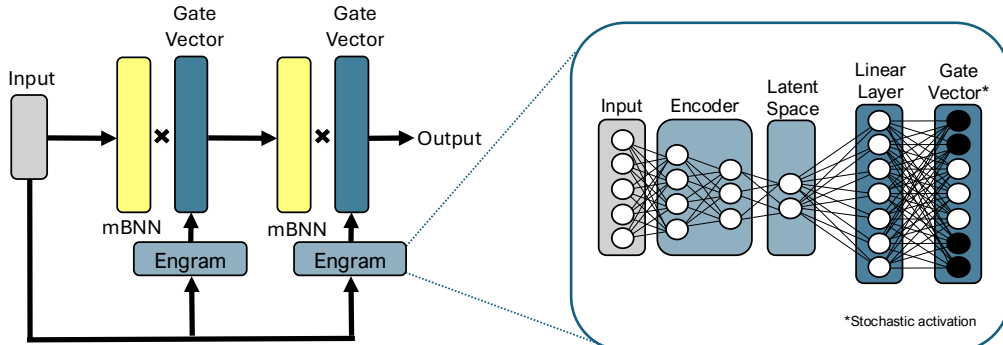


Figure 2: Engram block architecture. The engram block includes a two-layer encoder, one-layer latent space, one-layer linear layer, and a stochastic activation to output a gating vector to induce engrams for the metaplastic BNN.

Engram gating blocks that produce gating vectors to each metaplastic BNN (*mBNN*) hidden layer are supplied with the input dataset during training. This results in our unique engramBNN method. The model’s engram block, illustrated in Fig. 2, consists of a two-layer-wide fully-connected encoder that projects onto a lower dimension, aka. *the latent space*. This reduces the input to a compact representation where essential features are extracted. These semantic features serve as the spatial context that will inform engram formation. The latent space is connected to a linear layer used for knowledge recall [40].

A stochastic sign activation initiates the engrams that make up the subsequently active hidden neurons. The activations are defined by a Bernoulli distribution (Equ. 2), whose probability p is based on a sigmoid function of the hidden weight W_h , as shown in Equ. 1. The resulting weight, W_s is also a form of binary weight, valued at either 0 or +1 [36].

$$p = \sigma(z) = \frac{1}{1+e^{-W_h}} \quad (1)$$

$$W_s \sim \text{Bernoulli}(p) \quad (2)$$

The resulting vector is multiplied by each hidden layer, which serves as the gating mechanism for the *mBNN*. Regarding the architecture, each layer is a fully connected feedforward layer. The number of neurons per layer within the block is as follows: 512, 128, 64, 2048, and 2048 neurons.

2.3. Metaplasticity Function

Artificial metaplasticity is implemented to imitate synaptic plasticity and metaplasticity to reduce the effects of catastrophic forgetting. The implementation of metaplasticity in ANNs has been proven to be a powerful asset to continual learning [41, 42]. A function of metaplasticity, introduced by Laborieux *et al.* [42], is defined in Equ. 3, the hyperparameter m controls the network’s tendency to consolidate weights towards a task which, in turn, affects its sensitivity to new data. W_h is the real-valued hidden weight, whose absolute value signifies synaptic importance. In other words, as $|W_h|$ increases, it is more difficult to flip the binary sign of the synapse. A detailed breakdown of the metaplastic weight updates made is outlined in Appendix A.

$$f_{\text{meta}}(m, W_h) = 1 - \tanh^2(m \cdot W_h) \quad (3)$$

The learning rate was set to $\eta = 10^{-4}$ during training. Adam’s beta values (β_1, β_2) are (0.9, 0.999), respectively, as the default values.

2.4. Domain-Incremental Learning Experiments

Continual learning encompasses various incremental learning types: domain-incremental, class-incremental, and task-incremental learning. Each addresses different challenges in adapting to new data distributions. In domain-incremental learning, the input distribution shifts over time while the task and output targets remain unchanged. This differs from class-incremental learning, where new categories are introduced sequentially, and task-incremental learning, where new tasks require distinct boundaries. Here, we evaluate both domain and class-incremental computer vision experiments to assess the robustness of our model to various dataset biases and environmental shifts.

The most notable domain-incremental benchmark task is the Permuted-MNIST task [6]. In this scenario, the model must learn various permutations of the MNIST image dataset sequentially. Each task has a unique and random spatial permutation of pixels. Here, we argue that although it has been widely used in the continual learning field, Permuted-MNIST possesses fundamental flaws that make it an unreliable indicator of continual learning ability. There has been previous criticisms of Permuted-MNIST as it does not translate to real-world scenarios, and is at best a toy problem that does not capture the true nature of realistic domain shifts [43]. We present

Permuted-MNIST results in Appendix B to examine our model under a simple domain-incremental task.

Instead, we test our model on the more realistic CORE50-NI tasks, a specific experimental setting of the CORE50 dataset, whose domain shift is defined by varying backgrounds, lighting, poses, and occlusions [37]. The CORE50-NI dataset was captured in 11 sessions with unique backgrounds and lighting. The model is trained in eight sessions and tested on the remaining three. The model is trained for 20 epochs per task. We increase the number of hidden layer neurons from 2048 to 4096. Additionally, the number of neurons in the engram gating block is adjusted so that the last layer has 4096 neurons. The performance of the models is evaluated during the whole training on the test set.

2.5. Class-Incremental Learning Experiments

Another test for lifelong learning is class-incremental learning. Here, classes are introduced incrementally. The Split-MNIST experiment divides the standard MNIST dataset into a sequence of tasks, each containing a distinct subset of classes. Following the typical baseline setup, our test consists of five tasks, each introducing two new classes that have not been previously seen. Each unique task is fed to the model sequentially for 20 epochs. Similarly to domain-incremental experiments, although there are distinct tasks set up, task IDs are not provided to the model, meaning that our model is unaware when these tasks shift from one to the other.

For both domain- and class-incremental experiments, our model, termed engramBNN ($m = 5$ for Split-MNIST, $m = 175$ for CORE50-NI), is tested and compared to a baseline vanilla BNN. Continual learning baselines are also compared with our model and applied to the BNN architecture. We examine the performance of a metaplastic BNN (m BNN) (same m values as engramBNN), context-dependent gated BNN (XdG), and BNN with learning without forgetting (LwF). Additionally, recent biologically inspired state-of-the-art methods are tested, a hybrid neural network based on cortico-hippocampal recurrent loops (CH-HNN) and a sparsely distributed memory multilayer perceptron based on the cerebellum (SDMLP). The CH-HNN model is excluded from domain-incremental learning experiments, as it requires pre-trained ANN models and embeddings for CORE50 that were not available from the original experiments. Both state-of-the-art methods are not binarized, as preliminary experiments demonstrated a loss of all learning ability when linear layers were replaced with binarized layers.

2.6. Performance Measures

2.6.1. Continual Learning Metrics

In lifelong learning settings, the earlier performance metrics are further specified in the cumulative and final point versions. Average accuracy (ACC) is reported. As shown in Equ. 4, ACC takes the final accuracy, $A_{i,t}$, for each task t and averages them over the number of tasks seen. This gives a task-wise view of learning retention of the continual learning network.

$$\text{ACC} = \frac{1}{T} \sum_{i=1}^T A_{T,i} \quad (4)$$

A weighted accuracy value (weighted ACC, $w\text{ACC}$) is also calculated. Presented in Equ. 5, the final accuracy for each task is weighted, so older tasks have more importance than normalized over the sum of weights.

The weight is signified by an exponential function ($w_i = e^{\lambda t_i}$), which ensures gradual changes in importance where older tasks are weighted more heavily than recent tasks to prioritize long-term retention of past information.

$$w\text{ACC} = \frac{\sum_{i=1}^T w_i A_{T,i}}{\sum_{i=1}^T w_i} . \quad (5)$$

Peak GPU usage and peak RAM usage in percentage are also reported to assess the network efficiency. This measure records the highest total power capacity consumption of the GPU and CPU for training each model. Considering this in the context of resource efficiency in edge devices and for real-world deployment is crucial.

Forward transfer (FWT) and backward transfer (BWT) are also continual learning metrics that evaluate learning and forgetting, respectively [10]. FWT examines forward knowledge transfer and evaluates a model’s ability to generalize learning from past tasks to future ones. It is defined as:

$$\text{FWT} = \frac{1}{T-1} \sum_{i=2}^T (A_{i,i} - A_{0,i}) . \quad (6)$$

BWT quantifies how previous task knowledge improves or is forgotten when learning on subsequent tasks. It is defined as:

$$\text{BWT} = \frac{1}{T-1} \sum_{i=1}^{T-1} (A_{T,i} - A_{i,i}) . \quad (7)$$

A positive BWT signifies improved knowledge when learning new tasks, while a negative BWT signifies knowledge deterioration. As it is standard behavior for models to show catastrophic forgetting, we also add a modified metric based on BWT, known as Remembering (REM). Remembering or $REM = 1 - |\min(BWT, 0)|$.

3. Results

3.1. Split-MNIST

With the class-incremental Split-MNIST task, engramBNN performed better than the continual learning baselines and the state-of-the-art regarding accuracy. In Fig. 3(a), final test accuracies are reported across all five tasks, where engramBNN can maintain higher accuracy for almost all models without significant variance. EngramBNN also maintains higher accuracy as new tasks are introduced, as shown in Fig. 3(b). Although the state-of-the-art methods CH-HNN and SDMLP show higher final test accuracy for specific tasks, their average test accuracy is also significantly lower than engramBNN and shows more significant deviation across runs.

Table 1: Split-MNIST continual learning metrics. Average results are reported along with their standard deviations.

Model	ACC	$wACC^*$	FWT	BWT	REM
engramBNN ($m = 5$)	0.27±0.01	0.19±0.02	0.01±0.03	-0.64±0.05	0.37±0.05
Vanilla BNN ($m = 0$)	0.15±0.00	0.08±0.00	0.05±0.03	-0.70±0.04	0.29±0.04
LwF	0.20±0.04	0.12±0.04	0.04±0.01	-0.65±0.05	0.35±0.05
XdG	0.19±0.02	0.14±0.03	0.04±0.03	-0.52±0.04	0.48±0.04
$mBNN$ ($m = 5$)	0.19±0.05	0.12±0.04	0.04±0.04	-0.65±0.05	0.35±0.05
SDMLP	0.14±0.06	0.10±0.04	0.00±0.00	-0.53±0.36	0.47±0.36
CH-HNN	0.12±0.03	0.11±0.04	0.05±0.02	-0.11±0.10	0.89±0.10

For each model, all performance results are averaged over six training runs. The best values are in bold. $*wACC$: weighted ACC.

In Table 1, the engramBNN method had both higher ACC and Weighted ACC at 0.27 and 0.19, respectively. CH-HNN demonstrated better retention of old knowledge with a higher BWT and REM score. However, as seen in Fig. 3(b), the accuracy retained is low within the 10-40% neighborhood. The vanilla BNN also surprisingly had the highest recorded FWT

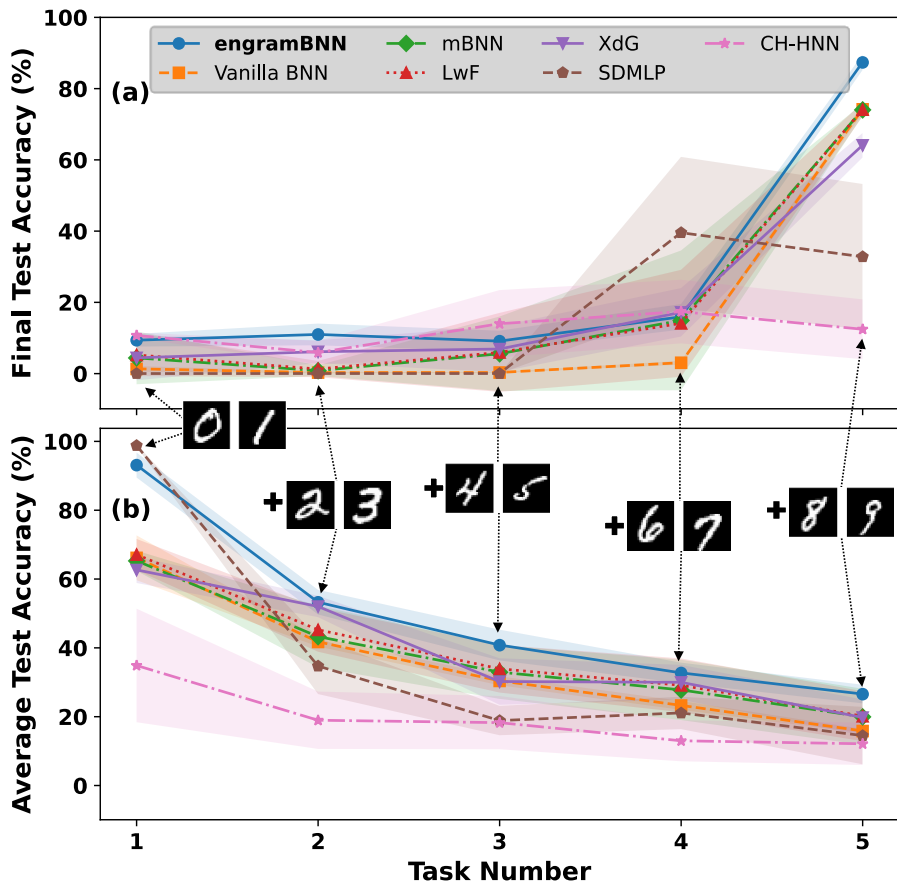


Figure 3: **Test accuracies on Split-MNIST.** In Split-MNIST, two additional and unseen classes are introduced to the model for every sequential task. **(a)** Final test accuracies across five tasks in the Split-MNIST setting. Averaged over six runs, the solid curves are the training results for 20 epochs per task. The shaded areas represent the standard deviation. **(b)** The average test accuracy over each task.

score, implying that it is capable of zero-shot learning. However, considering that the FWT scores of all models are under 0.05, it is unlikely that this is meaningful, as it may result from factors such as random initialization, or the limited representational capacity of the BNN.

3.2. CORE50-NI

In the domain-incremental setting, we use the CORE50-NI experiment. As presented in Table 2, although vanilla BNN had the highest recorded

ACC, our engramBNN model had the highest weighted ACC of 0.19. Our model also had the highest FWT score of 0.16 and the second-best BWT and REM scores falling behind the state-of-the-art SDMLP.

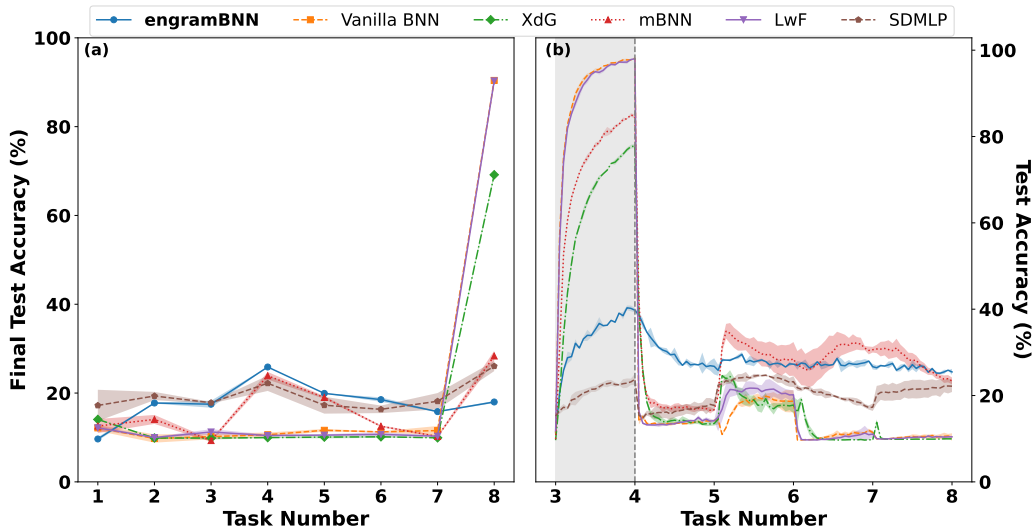


Figure 4: **Test accuracies on CORE50-NI.** (a) Final test accuracies across eight tasks in CORE50. Averaged over three runs, solid curves represent the test accuracy, where each task has been trained for 20 epochs. Shaded areas represent one standard deviation. (b) Test accuracy of the third task in the CORE50-NI, experiment. The shaded gray area represents the learning phase of the models, which is cut off by a gray dotted line.

Table 2: CORE50-NI continual learning metrics. Average values are reported along with their respective standard deviations.

Model	ACC	$wACC^*$	FWT	BWT	REM
engramBNN ($m = 175$)	0.18±0.00	0.19±0.00	0.16±0.00	-0.17±0.15	0.83±0.15
Vanilla BNN ($m = 0$)	0.20±0.00	0.12±0.00	0.14±0.00	-0.83±0.03	0.20±0.03
LwF	0.19±0.00	0.11±0.00	0.12±0.00	-0.82±0.03	0.22±0.03
XdG	0.18±0.00	0.10±0.00	0.11±0.00	-0.56±0.05	0.24±0.05
mBNN ($m = 175$)	0.16±0.00	0.15±0.00	0.13±0.00	-0.54±0.20	0.23±0.20
SDMLP	0.18±0.01	0.18±0.01	0.13±0.01	-0.04±0.03	0.96±0.03

For each model, all performance results are averaged over six training runs. The best values are in bold. * $wACC$: weighted ACC.

In Fig. 4(a), the engramBNN model maintains a higher accuracy for most tasks, especially compared to continual learning baselines. When tested against the SDMLP model, final test accuracy is comparable, but more variance is exhibited, suggesting less stability. Fig. 4(b) shows the test accuracy of the third task in the CORE50 setting. The vanilla BNN, m BNN, LwF, and XdG all demonstrate extreme catastrophic forgetting after learning on task 3 (learning occurs in the gray shaded region). Only the engramBNN and SDMLP have limited forgetting effects, whereas the engramBNN maintains higher accuracy throughout the remaining experiment. The m BNN performance also improves but is unstable compared to other methods. At the point in which the last task is being fully learned, the vanilla BNN, XdG, and LwF models are no better than random chance.

3.3. System Performance Metrics

The peak GPU and RAM usage was also recorded during the Split-MNIST experiment and are presented in Table 3. For GPU usage, the engramBNN had the lowest utilization at 4.51%. The CH-HNN model had the lowest RAM process usage, equal to 19.51%. Both models demonstrated higher efficiency compared to all other models. The model with the highest GPU usage was LwF, at 12.39%. The SDMLP had the highest RAM usage at 26.61%.

Table 3: System performance metrics. Measurements were taken from the Weights and Biases (WandB [44]) system metric documentation, which is logged every 10 seconds. The total GPU memory is approximately 17 GB.

Model	Peak GPU Usage (%)	Peak RAM Usage (%)
engramBNN ($m = 5$)	4.51	19.51
Vanilla BNN ($m = 0$)	7.95	21.18
LwF	12.39	25.71
XdG	8.47	22.30
m BNN ($m = 5$)	8.46	22.31
SDMLP	7.30	26.61
CH-HNN	4.54	16.98

4. Discussion

Metaplasticity and probabilistic context-dependent gating inform artificial engrams in a resource-efficient BNN architecture. Our model was tested on a class and domain-incremental learning setting on image-based data. Both tests demonstrated comparable performance with the previously validated metaplastic BNN, surpassing GPU efficiency in baseline and vanilla models.

The combination of context-dependent gating and metaplasticity provides a meaningful solution to continual learning by enabling more flexible and adaptive learning mechanisms. Context-dependent gating informs artificial engrams inspired by the biological memory traces representing learned information. When induced by stochastic activations, these engrams improve the network’s ability to adapt to new tasks in a dynamic learning environment. Probabilistic activations induce engrams through their stochastic approach, allowing for more knowledge retention. The metaplasticity mechanism further adjusts synaptic plasticity based on prior learning, allowing the model to prevent task interference better. Together, these processes enable more stable learning and contribute to developing power-efficient systems with their binarized architecture, making them suitable for real-world lifelong learning applications where resources are constrained.

Our model showed superior performance in the class-incremental experiment, with better performance than the vanilla models, baselines, and state-of-the-art continual learning methods, and significantly reduced resource usage, utilizing less than half the GPU power consumption compared to other networks. In edge computing and real-time applications, consideration of resource efficiency is critical. The probabilistic activation of engram formation helped facilitate this stable and scalable learning, contributing to the overall effectiveness of the model.

In this study, we also focused on a domain-incremental setting to evaluate the model’s ability to learn and retain knowledge from a changing data distribution. We strongly believe that Permuted-MNIST is ineffective as a continual learning benchmark. The reason it is referred to here is its prevalent use. We employed the CORe50 dataset as a realistic alternative to address the need for a more realistic dataset. This benchmark posed challenges, as the images were more complex and had eleven different scenarios with varying backgrounds and lighting. Our model had improved weighted accuracy over other models and exhibited forward transfer abilities.

EngramBNN can continually learn in the domain-incremental setting, as evident in its FWT and BWT scores. However, it struggles to capture the complexity of RGB images of diverse objects. This may be addressed by employing different architectures as the backbone of our model, such as low-power CNNs, SNNs, or energy-based models [45]. However, it should be acknowledged that there is a tradeoff between efficiency, power consumption, and performance in achieving the low power requirements for edge devices.

The experiments are task-agnostic because they do not require a task ID explicitly provided to the model (except for the XdG method, which requires this for all scenarios). Although we did not explore new strategies for real-time label generation or incorporate a noisy student approach here, we acknowledge that this is an important direction for future studies. Incorporating methods such as noisy student labeling or weak- or pseudo-labeling [46] could potentially overcome this limitation but requires careful consideration of the trade-offs between computational efficiency and accuracy in such settings.

Inspired by mechanisms introduced in metaplasticity and context-dependent gating methods, our model demonstrates improved accuracy and lower resource consumption. Leveraging these helped facilitate a biologically plausible mechanism for lifelong learning. Furthermore, our method is closely related to the recently published CH-HNN method, which was compared in our experiments. Both approaches employ metaplasticity and induce some gating to modulate the signal. However, we argue that our approach is more efficient on the backend, as it eliminates the need for pre-training and computing similarities for modulation signals. Unlike the CH-HNN, which necessitates the hybridization of an ANN and SNN, our method simplifies the process while achieving similar, if not improved, results.

Our model has demonstrated a promising approach to tackle the challenges of resource-efficient continual learning. By incorporating biological mechanisms, we achieved superior efficiency with competitive performance in class and domain-incremental setups. While these results are encouraging, future work will address the limitations of supervised learning in these environments. Further investigations will focus on refining the gating mechanism and exploring its impact in more complex, real-world environments, such as with brain signals. Ultimately, this work lays the foundation for more adaptive, efficient, and scalable models suitable for deployment in edge computing and dynamic learning environments.

Acknowledgements

The authors acknowledge the support from the Australian Research Council under Project DP230100019. I.A. acknowledges support for the Australian Government’s Research Training Program (RTP). L.F.H.C. acknowledges partial support from The University of Sydney.

Code Availability

Any related questions regarding the code supporting the findings of this study can be directed to the corresponding author.

Data Availability

We employed publicly accessible datasets. They can be accessed via

- MNIST: <http://yann.lecun.com/exdb/mnist/>, and
- CORe50: <https://vlomonaco.github.io/core50/>.

Conflicts of Interest

All authors declare that they have no conflicts of interest to disclose.

Appendix A. Metaplastic Optimization Algorithm

Algorithm 1 Hidden weight metaplastic update for BNN, described in our previous work in [41]. \mathbf{W}_h is the vector of real-valued hidden weights, and W_h denotes one element (as applied to all other vectors involved), \mathbf{U}_w is the weight update, (x,y) is a batch of labeled training data, m is the metaplasticity parameter, and η is the learning rate.

Require: $\mathbf{W}_h, (x, y), \mathbf{U}_w, \eta, m$

```

1:  $\mathbf{W}_b \leftarrow \text{Sign}(\mathbf{W}_h)$  ▷ Computing binary weights
2:  $\hat{y} \leftarrow \text{Forward}(x, \mathbf{W}_b)$  ▷ Perform inference
3:  $C \leftarrow \text{Cost}(\hat{y}, y)$  ▷ Compute mean loss over the batch
4:  $\mathbf{U}_w \leftarrow \text{Adam Backward}(C, \mathbf{W}_b, \mathbf{U}_w, \hat{y})$  ▷ Compute backward update with the binarized weights
5: if  $U_w \cdot W_b > 0$  then ▷ For a single weight if  $U_w$  prescribes to decrease  $|W_h|$ 
6:    $W_h \leftarrow W_h - \eta \mathbf{U}_w \cdot f_{\text{meta}}(m, W_h)$  ▷ Metaplastic update
7: else
8:    $W_h \leftarrow W_h - \eta \mathbf{U}_w$ 
9: end if
10: return  $W_h, U_w$ 

```

Appendix B. Permuted-MNIST Experiments

Here, we present results from the domain-incremental Permuted-MNIST task. Here, the SDMLP method showed higher accuracy performance and backward transfer-related scores, as shown in Table B.4. Our engramBNN model showed slightly higher forward transfer ability than all other methods.

We believe that the SDMLP showed a more significant advantage due to its use of fully connected linear layers in its architecture, as opposed to our binarized layers, allowing more precise weight updates and greater representational capacity, which likely contributed to its improved performance. We remained comparable in performance to the hybrid CH-HNN model, which employs SNN and fully connected ANN architectures.

Table B.4: Permuted-MNIST continual learning metrics. All values are averages plus or minus their standard deviations.

Model	ACC	$w\text{ACC}^*$	FWT	BWT	REM
engramBNN ($m = 5$)	0.53±0.01	0.36±0.01	0.11±0.01	-0.45±0.20	0.55±0.20
Vanilla BNN ($m = 0$)	0.46±0.01	0.25±0.02	0.10±0.01	-0.54±0.25	0.46±0.25
LwF	0.47±0.01	0.25±0.02	0.10±0.01	-0.53±0.26	0.48±0.26
XdG	0.57±0.01	0.40±0.02	0.11±0.01	-0.34±0.20	0.66±0.20
m BNN ($m = 5$)	0.49±0.01	0.30±0.02	0.10±0.01	-0.49±0.24	0.52±0.24
SDMLP	0.63±0.01	0.56±0.02	0.09±0.01	-0.15±0.10	0.85±0.10
CH-HNN	0.50±0.01	0.35±0.03	0.10±0.01	-0.46±0.18	0.54±0.18

For each model, all performance results are averaged over six training runs. The best values are in bold. * $w\text{ACC}$: weighted ACC.

References

- [1] Ikhwan Jeon and Taegon Kim. Distinctive properties of biological neural networks and recent advances in bottom-up approaches toward a better biologically plausible neural network. *Frontiers in Computational Neuroscience*, 17:1092185, 2023.
- [2] Raia Hadsell, Dushyant Rao, Andrei A Rusu, and Razvan Pascanu. Embracing change: Continual learning in deep neural networks. *Trends in Cognitive Sciences*, 24(12):1028–1040, 2020.
- [3] Peter Jedlicka, Matus Tomko, Anthony Robins, and Wickliffe C Abraham. Contributions by metaplasticity to solving the catastrophic forgetting problem. *Trends in Neurosciences*, 45(9):656–666, 2022.
- [4] Liyuan Wang, Xingxing Zhang, Hang Su, and Jun Zhu. A comprehensive survey of continual learning: Theory, method and application. *IEEE Transactions on Pattern Analysis and Machine Intelligence*, 46(8):5362–5383, 2024.
- [5] James Kirkpatrick, Razvan Pascanu, Neil Rabinowitz, Joel Veness, Guillaume Desjardins, Andrei A Rusu, Kieran Milan, John Quan, Tiago Ramalho, Agnieszka Grabska-Barwinska, et al. Overcoming catastrophic forgetting in neural networks. *Proceedings of the National Academy of Sciences*, 114(13):3521–3526, 2017.

- [6] Friedemann Zenke, Ben Poole, and Surya Ganguli. Continual learning through synaptic intelligence. *International Conference on Machine Learning*, pages 3987–3995, 2017.
- [7] Zhizhong Li and Derek Hoiem. Learning without forgetting. *IEEE Transactions on Pattern Analysis and Machine Intelligence*, 40(12):2935–2947, 2017.
- [8] Guido M Van de Ven, Hava T Siegelmann, and Andreas S Tolias. Brain-inspired replay for continual learning with artificial neural networks. *Nature Communications*, 11(1):4069, 2020.
- [9] Sylvestre-Alvise Rebuffi, Alexander Kolesnikov, Georg Sperl, and Christoph H Lampert. iCaRL: Incremental classifier and representation learning. *Proceedings of the IEEE Conference on Computer Vision and Pattern Recognition*, pages 2001–2010, 2017.
- [10] David Lopez-Paz and Marc’Aurelio Ranzato. Gradient episodic memory for continual learning. *Advances in Neural Information Processing Systems*, 30, 2017.
- [11] Arun Mallya, Dillon Davis, and Svetlana Lazebnik. Piggyback: Adapting a single network to multiple tasks by learning to mask weights. *Proceedings of the European Conference on Computer Vision (ECCV)*, pages 67–82, 2018.
- [12] Arun Mallya and Svetlana Lazebnik. Packnet: Adding multiple tasks to a single network by iterative pruning. *Proceedings of the IEEE Conference on Computer Vision and Pattern Recognition*, pages 7765–7773, 2018.
- [13] Guanxiong Zeng, Yang Chen, Bo Cui, and Shan Yu. Continual learning of context-dependent processing in neural networks. *Nature Machine Intelligence*, 1(8):364–372, 2019.
- [14] Khurram Javed and Martha White. Meta-learning representations for continual learning. *Advances in Neural Information Processing Systems*, 32, 2019.

- [15] Divyam Madaan, Jaehong Yoon, Yuanchun Li, Yunxin Liu, and Sung Ju Hwang. Representational continuity for unsupervised continual learning. *arXiv preprint arXiv:2110.06976*, 2021.
- [16] Wickliffe C Abraham and Mark F Bear. Metaplasticity: The plasticity of synaptic plasticity. *Trends in Neurosciences*, 19(4):126–130, 1996.
- [17] Wickliffe C Abraham. Metaplasticity: Tuning synapses and networks for plasticity. *Nature Reviews Neuroscience*, 9(5):387–387, 2008.
- [18] Axel Guskjolen and Mark S Cembrowski. Engram neurons: Encoding, consolidation, retrieval, and forgetting of memory. *Molecular Psychiatry*, 28(8):3207–3219, 2023.
- [19] Leon G Reijmers, Brian L Perkins, Naoki Matsuo, and Mark Mayford. Localization of a stable neural correlate of associative memory. *Science*, 317(5842):1230–1233, 2007.
- [20] Kaycie K Tayler, Kazumasa Z Tanaka, Leon G Reijmers, and Brian J Wiltgen. Reactivation of neural ensembles during the retrieval of recent and remote memory. *Current Biology*, 23(2):99–106, 2013.
- [21] Edward A Wasserman and Ralph R Miller. What’s elementary about associative learning? *Annual Review of Psychology*, 48(1):573–607, 1997.
- [22] Richard F Thompson, Shaowen Bao, Lu Chen, Benjamin D Cipriano, Jeffrey S Grethe, Jeansok J Kim, Judith K Thompson, Jo Anne Tracy, Martha S Weninger, and David J Krupa. Associative learning. *International Review of Neurobiology*, 41:151–189, 1997.
- [23] James B Heald, Daniel M Wolpert, and Máté Lengyel. The computational and neural bases of context-dependent learning. *Annual Review of Neuroscience*, 46(1):233–258, 2023.
- [24] Samuel J Gershman. A unifying probabilistic view of associative learning. *PLoS Computational Biology*, 11(11):e1004567, 2015.
- [25] Hans Liljenström and X-B Wu. Noise-enhanced performance in a cortical associative memory model. *International Journal of Neural Systems*, 6(01):19–29, 1995.

- [26] Xibin Dong, Zhiwen Yu, Wenming Cao, Yifan Shi, and Qianli Ma. A survey on ensemble learning. *Frontiers of Computer Science*, 14:241–258, 2020.
- [27] Christos Louizos, Max Welling, and Diederik P Kingma. Learning sparse neural networks through l_0 regularization. *International Conference on Learning Representations*, 2017.
- [28] Nitish Srivastava, Geoffrey Hinton, Alex Krizhevsky, Ilya Sutskever, and Ruslan Salakhutdinov. Dropout: A simple way to prevent neural networks from overfitting. *The Journal of Machine Learning Research*, 15(1):1929–1958, 2014.
- [29] Sinno Jialin Pan and Qiang Yang. A survey on transfer learning. *IEEE Transactions on Knowledge and Data Engineering*, 22(10):1345–1359, 2009.
- [30] Daniel S Rizzuto and Michael J Kahana. An autoassociative neural network model of paired-associate learning. *Neural Computation*, 13(9):2075–2092, 2001.
- [31] Charlie Tang and Russ R Salakhutdinov. Learning stochastic feedforward neural networks. *Advances in Neural Information Processing Systems*, 26, 2013.
- [32] Nicolas Y Masse, Gregory D Grant, and David J Freedman. Alleviating catastrophic forgetting using context-dependent gating and synaptic stabilization. *Proceedings of the National Academy of Sciences*, 115(44):E10467–E10475, 2018.
- [33] Matthew James Tilley, Michelle Miller, and David Freedman. Artificial neuronal ensembles with learned context dependent gating. *The Eleventh International Conference on Learning Representations*, 2023.
- [34] Matthieu Courbariaux, Yoshua Bengio, and Jean-Pierre David. Binaryconnect: Training deep neural networks with binary weights during propagations. *Advances in Neural Information Processing Systems*, 28, 2015.
- [35] Francesco Conti, Pasquale Davide Schiavone, and Luca Benini. XNOR neural engine: A hardware accelerator IP for 21.6-fJ/op binary neural

- network inference. *IEEE Transactions on Computer-Aided Design of Integrated Circuits and Systems*, 37(11):2940–2951, 2018.
- [36] Itay Hubara, Matthieu Courbariaux, Daniel Soudry, Ran El-Yaniv, and Yoshua Bengio. Binarized neural networks. *Advances in Neural Information Processing Systems*, 29, 2016.
- [37] Vincenzo Lomonaco and Davide Maltoni. CORE50: a new dataset and benchmark for continuous object recognition. *Conference on Robot Learning*, pages 17–26, 2017.
- [38] Taylor Simons and Dah-Jye Lee. A review of binarized neural networks. *Electronics*, 8(6):661, 2019.
- [39] Mohammad Rastegari, Vicente Ordonez, Joseph Redmon, and Ali Farhadi. XNOR-Net: Imagenet classification using binary convolutional neural networks. *European Conference on Computer Vision*, pages 525–542, 2016.
- [40] Liliang Ren, Yang Liu, Yadong Lu, yelong shen, Chen Liang, and Weizhu Chen. Samba: Simple hybrid state space models for efficient unlimited context language modeling. *The Thirteenth International Conference on Learning Representations*, 2025.
- [41] Isabelle Aguilar, Thomas Bersani-Veroni, Luis Fernando Herbozo Contreras, Armin Nikpour, Damien Querlioz, and Omid Kavehei. Continuous metaplastic training on brain signals. *npj Unconventional Computing*, 2025.
- [42] Axel Laborieux, Maxence Ernout, Tifenn Hirtzlin, and Damien Querlioz. Synaptic metaplasticity in binarized neural networks. *Nature Communications*, 12(1):2549, 2021.
- [43] Sebastian Farquhar and Yarin Gal. Towards robust evaluations of continual learning. *Lifelong Learning: A Reinforcement Learning Approach Workshop, ICML, 2018*, 2018.
- [44] Experiment Tracking with Weights & Biases: The AI Developer Platform. <https://www.wandb.com>, 2025. [Accessed 24-03-2025].

- [45] Shuang Li, Yilun Du, Gido Van de Ven, and Igor Mordatch. Energy-based models for continual learning. *Conference on Lifelong Learning Agents*, pages 1–22, 2022.
- [46] Qizhe Xie, Minh-Thang Luong, Eduard Hovy, and Quoc V Le. Self-training with noisy student improves ImageNet classification. *Proceedings of the IEEE/CVF Conference on Computer Vision and Pattern Recognition*, pages 10687–10698, 2020.